

Low Energy Solar Neutrinos and Spin Flavour Precession

Bhag C. Chauhan*, João Pulido†

CENTRO DE FÍSICA TEÓRICA DAS PARTÍCULAS (CFTP)

Departamento de Física, Instituto Superior Técnico

Av. Rovisco Pais, P-1049-001 Lisboa, Portugal

and

R. S. Raghavan‡

Department of Physics

Virginia Polytechnic Institute and State University (Virginia Tech)

Blacksburg VA 24060 USA

Abstract

The possibility that the Gallium data effectively indicates a time modulation of the solar active neutrino flux in possible connection to solar activity is examined on the light of spin flavour precession to sterile neutrinos as a subdominant process in addition to oscillations. We distinguish two sets of Gallium data, relating them to high and low solar activity. Such modulation affects principally the low energy neutrinos (pp and ${}^7\text{Be}$) so that the effect, if it exists, will become most clear in the forthcoming Borexino and LENS experiments and will provide evidence for a neutrino magnetic moment. Using a model previously developed, we perform two separate fits in relation to low and high activity periods to all solar neutrino data. These fits include the very recent charged current spectrum from the SNO experiment. We also derive the model predictions for Borexino and LENS experiments.

*On leave from Govt. Degree College, Karsog (H P) India 171304. E-mail: chauhan@cftp.ist.utl.pt

†E-mail: pulido@cftp.ist.utl.pt

‡E-mail: raghavan@vt.edu

1 Introduction and Motivation

The quest for time dependence of the solar neutrino flux and the development of low energy ($< 1\text{-}2$ MeV) solar neutrino experiments are probably at present the major challenges facing solar neutrino physics. Evidence for time variability has been found by the Stanford Group [1],[2],[3], [4], [5] upon examination of time binned data from all experiments except, so far, SNO. If it is confirmed, time variability will probably require neutrino spin flavor precession (SFP) [6] within the sun through the interaction of the neutrino magnetic moment with a varying solar magnetic field occurring in addition to the LMA effect. On the other hand the effort in real time experiments SuperKamiokande [7] and SNO [8] has been up to now concentrated in measuring the high energy ${}^8\text{B}$ flux which accounts for a fraction of 10^{-4} of the total solar neutrino flux. The important pp flux and the ${}^7\text{Be}$ one which together constitute more than 98% of the total flux have up to now been detected through the inclusive measurements of the radiochemical experiments SAGE [9], [10], Gallex/GNO [11],[12], [13]. Examination of the low energy solar neutrinos in particular the pp flux alone will teach us about the possible vacuum-matter transition, test the principle of nuclear energy generation in the sun and the luminosity condition [14]. For these reasons performing real time low energy solar neutrino experiments should at present be regarded as a major objective in the solar neutrino program [15].

Gallium experiments [11] are the only ones up to now in which neutrinos of energy below 1 MeV ($pp, {}^7\text{Be}$) account for a significant fraction ($\simeq 80\%$) of the event rate. Other experiments are unable to detect pp neutrinos, owing to the low threshold required (their energies lie below 0.42 MeV) while the ${}^7\text{Be}$ ones account for only 14% of the Chlorine event rate [13]. Therefore still very little is known about most of the neutrino flux from the sun. Nevertheless, as it has been recently noticed [16], [11], the average rate from the two Gallium experiments, SAGE and Gallex-GNO, has been evolving since the time they started in 1990-91 in such a way that the data from the periods 1991-97 and 1998-03 show a relative discrepancy of 2.4σ (see table I). It is tempting to establish a parallel between this fact and the solar magnetic activity. The first period was mainly a time of decreasing activity following a maximum which had taken place in mid-1990. It ended after the mid-1996 low at the initiation of a new solar cycle. For the whole period the average sunspot number was 52. In the second period the solar activity was stronger with a peak in the second quarter of 2000 and an average sunspot number of 100 [17]. While 2.4σ discrepancy is not compelling evidence of new physics, it certainly deserves close investigation, especially in view of the above stated fact that Gallium are the only experiments with an sizable contribution of $pp, {}^7\text{Be}$. Consequently, and since no other experiments show such a variational effect, the time dependence of these fluxes becomes an open possibility which we investigate in the present work. Long-term measurements with low energy solar neutrino detectors like the

forthcoming Borexino [18], dedicated to ${}^7\text{Be}$, and LENS [19],[20],[21] observing separately all low energy fluxes, can settle this question.

The present article aims at exploring and refining a model previously introduced [22] based on the joint effect of spin flavour precession to light sterile neutrinos and LMA. It will be seen that it can naturally lead to a time dependence of the low energy solar neutrino flux ($E < 2$ MeV) with special incidence on pp and ${}^7\text{Be}$. To this end the spin flavour resonance of these neutrinos must occur in the region where the field is the strongest, in the deep convective zone. Their amount of conversion is therefore expected to accompany the solar activity. As previously mentioned, the main motivation of the present analysis is provided by the Gallium data apparent variability and a clear test of the model by the future Borexino and LENS. We will therefore present the model predictions for these experiments.

The article is structured as follows: in section 2 we review the essentials of the model, referring the reader to [22] for details. In section 3 we examine Gallium data assumed to be modulated as in table I. We consider two options: (a) modulation to be principally due to time dependent pp neutrino conversion and (b) shared between pp and ${}^7\text{Be}$ neutrino conversion. Restricting the oscillation parameters $\Delta m_{21}^2, \theta$ within their 1σ ranges [23], we determine the values of Δm_{10}^2 (active/sterile mass squared difference), f_B (${}^8\text{B}$ flux normalization) and field profile which provide the best fits separately in each option. All convenient field profiles are expected to exhibit a time varying peak in the tachocline correlated with solar activity. In the active period (1998-03) the data favour a field profile with an average peak value in the range (220-250) kG. For the other, semiquiet period (1991-97), this decreases to (30-50) kG with a similar profile being favoured. In section 4 we develop the predictions for Borexino and LENS assuming the time dependent field profile anchored in the tachocline as derived from options (a) and (b). In Borexino the first scenario (pp modulation dominance) will be more difficult to detect, as expected, while the second could provide a clear signature. In LENS both cases are visible in each energy sector. Finally in section 5 we draw our perspectives and main conclusions, ending with a discussion of prospects of active \rightarrow sterile conversion for supernova dynamics.

| Period | 1991-97 | 1998-03 |
|----------------|----------------|----------------|
| SAGE+Ga/GNO | 77.8 ± 5.0 | 63.3 ± 3.6 |
| Ga/GNO only | 77.5 ± 7.7 | 62.9 ± 6.0 |
| no. of suspots | 52 | 100 |

Table I - Average rates for Ga experiments and average number of sunspots in the same periods [17] (units are SNU).

2 Summary of the Model

The starting point of our present work is a model previously developed based on LMA with two flavours in which a light sterile neutrino is added [22]. Its original motivations are the three apparent problems with LMA: inability to explain the possible time variability of the neutrino event rate, the predicted upturn of the electron spectrum in SuperKamiokande (unobserved by experiment) and the prediction for the Cl rate (2.9-3.1 SNU) which is about 2σ too high. Decreasing the Cl rate prediction together with providing a flat spectrum instead of an upturned one implies a change in the LMA survival probability. The modified probability should exhibit a dip in the low/intermediate neutrino energies. Moreover the conversion from active to sterile state proceeds through resonant spin flavour precession (RSFP) determined by a magnetic field profile located mainly nearly the bottom of the convective zone of the sun. The two resonances (LMA and RSFP) therefore occur at very different solar densities (LMA in the core, RSFP in the convective zone) and the 'new' mass squared difference between neutrino flavors is $O(10^{-8}eV^2)$ in order to provide for the RSFP resonance at the correct location. This choice is not only consistent with dynamo theories [24], which predict a strong field in the deep convective zone, but also precludes interference between the two resonances, thus providing a clear and observable effect superimposed on the 'pure' LMA one. Since, for fixed mass squared difference, the neutrino energy determines the location of the resonance, the time dependent effect associated with a time varying field profile may affect some of the neutrino fluxes in detriment of others. The above magnitude of Δm^2 excludes conversion to active neutrinos, for which both known values of the mass square differences are larger. So we are lead to consider active \rightarrow sterile neutrino conversion. Furthermore, conversion of the original ν_e to an active antineutrino [25] (either $\bar{\nu}_\mu$ or $\bar{\nu}_\tau$) is highly disfavoured, since, owing to the large mixing angle, this antineutrino would oscillate to $\bar{\nu}_e$ on its way to the earth, leading to a large observable $\bar{\nu}_e$ flux. This effect, proposed years ago [26],[27],[28], will not be considered here, as a sizable $\bar{\nu}_e$ flux is ruled out by KamLAND for $E > 8MeV$ [29]. There are however no low energy limits for $\bar{\nu}_e$ flux from the sun.

In line with our previous work [22], we will consider at present the possibility of a time dependent active \rightarrow sterile transition. In the simplest such departure from the conventional LMA, the active and sterile sectors communicate through one magnetic moment transition only, with matter Hamiltonian [22]

$$\mathcal{H}_M = \begin{pmatrix} \frac{-\Delta m_{10}^2}{2E} & \mu_\nu B & 0 \\ \mu_\nu B & \frac{\Delta m_{21}^2}{2E} s_\theta^2 + V_e & \frac{\Delta m_{21}^2}{4E} s_{2\theta} \\ 0 & \frac{\Delta m_{21}^2}{4E} s_{2\theta} & \frac{\Delta m_{21}^2}{2E} c_\theta^2 + V_x \end{pmatrix} \quad (1)$$

in the mass matter basis $(\tilde{\nu}_0 \ \tilde{\nu}_1 \ \tilde{\nu}_2)$ to which corresponds the mixing

$$\begin{pmatrix} \nu_s \\ \nu_e \\ \nu_x \end{pmatrix} = \begin{pmatrix} 1 & 0 & 0 \\ 0 & c_\theta & s_\theta \\ 0 & -s_\theta & c_\theta \end{pmatrix} \begin{pmatrix} \nu_0 \\ \nu_1 \\ \nu_2 \end{pmatrix}. \quad (2)$$

in the vacuum basis $(\nu_0 \ \nu_1 \ \nu_2)$. In eqs.(1), (2) V_e, V_x are the matter induced potentials for ν_e and ν_x , θ is the vacuum mixing angle and $\Delta m_{10}^2 = m_1^2 - m_0^2$ is the mass squared difference between active and sterile states.

The important transition whose time dependent efficiency may determine the possible modulation of neutrino flux is therefore between mass matter eigenstates $\tilde{\nu}_0, \tilde{\nu}_1$. This is expected to resonate in the region where the magnetic field is the strongest in the period of high solar activity.

3 Examining Gallium data

We refer in this section to Ga data as given in table I, Cl data as in table II, the SuperKamiokande spectral data for 1496 days as in [7] and the SNO data as in [8]. Hence we consider time averaged data except for Ga which we split in two long term sets, namely the averages for 1991-97 (Ga I) and for 1998-03 (Ga II), in possible connection to the solar periodic activity. We perform statistical analyses for each Ga set together with all other solar data, examining in turn the case in which the flux modulation is determined mainly by pp neutrinos and the case in which the modulation dominance is shared by pp and ${}^7\text{Be}$. These should not however be regarded as two distinct cases, as they are connected by a continuous evolution of the parameter Δm_{10}^2 , any intermediate situation being equally viable. We consider parameters Δm_{21}^2 and θ to be fixed within the 1σ range of the KamLAND analysis [29]. Hence the 44 SuperKamiokande spectral data points, 34 SNO day/night charged current spectral rates, 4 SNO day/night electron scattering and neutral current rates, the Ga and Cl rates and 2 free parameters (Δm_{10}^2 , and the peak field value B_0), lead to 82 d.o.f. However, of these free parameters, the value of Δm_{10}^2 is fixed from a joint optimization of Ga I and Ga II fits. We evaluate in each case the global χ^2 (rates + spectrum) referring the reader to [30] for definitions. Our objective then consists in finding appropriate solar field profiles for each of the Ga data sets together with the other solar data which provide the best possible fits. The analysis is based on the general principle that an intense sunspot activity is correlated with a strong field located in the deep convective zone, while in the quiet sun period such field may disappear. Throughout the analysis we take $f_B = 1.0$, the neutrino magnetic moment $\mu_\nu = 10^{-12} \mu_B$, the LMA mass squared difference $\Delta m_{21}^2 = 8.3 \times 10^{-5} \text{eV}^2$ and vacuum mixing $\theta = 0.50$, thus within the KamLAND [29] allowed 1σ range, and we use the BS05(OP) standard solar model [31].

| Experiment | Data | Theory | Reference |
|------------|--|---------------------------|-----------|
| Homestake | $2.56 \pm 0.16 \pm 0.15$ | $8.09 \pm_{1.9}^{1.9}$ | [13] |
| SAGE | <i>see table I</i> | $125.9 \pm_{12.1}^{12.2}$ | [10] |
| Gallex+GNO | <i>see table I</i> | $125.9 \pm_{12.1}^{12.2}$ | [12] |
| SuperK | $2.35 \pm 0.02 \pm 0.08$ | 5.69 ± 1.41 | [7] |
| SNO CC | $1.68 \pm_{0.06}^{0.06} \pm_{0.09}^{0.08}$ | 5.69 ± 1.41 | [8] |
| SNO ES | $2.35 \pm_{0.22}^{0.22} \pm_{0.15}^{0.15}$ | 5.69 ± 1.41 | [8] |
| SNO NC | $4.94 \pm_{0.21}^{0.21} \pm_{0.34}^{0.38}$ | 5.69 ± 1.41 | [8] |

Table II - Data from the solar neutrino experiments except Ga which is given in Table I. Units are SNU for Homestake and $10^6 \text{cm}^{-2} \text{s}^{-1}$ for SuperKamiokande and SNO. We use the BS05(OP) solar standard model [31].

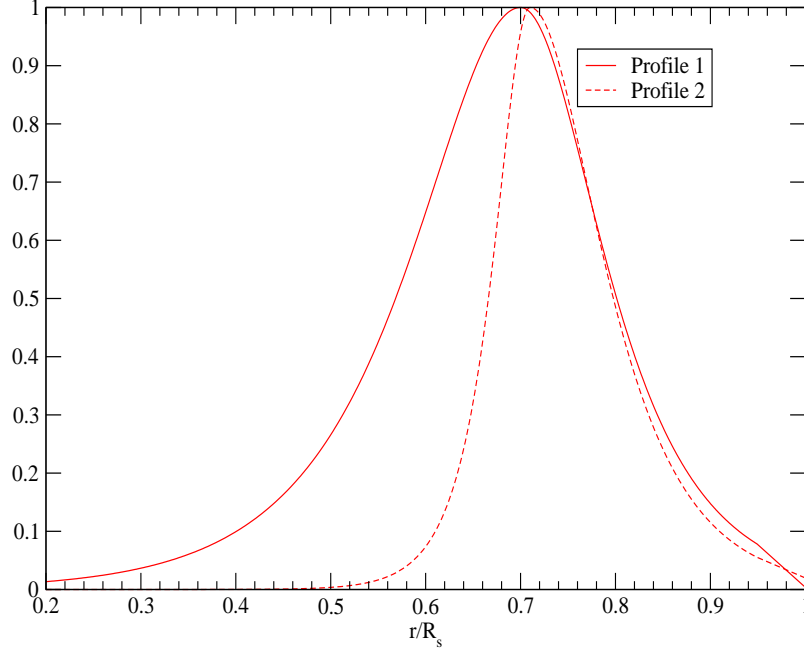


Figure 1: Normalized field profiles as a function of the solar coordinate $x = r/R_s$. Profile 1: eqs.(3), (4). Profile 2: eqs.(5), (6).

3.1 Modulation by pp

We start by considering the case where a time varying Ga rate is mainly due to pp modulation, implying therefore pp resonances to lie in the region of a time varying field peak. Since this is expected to be located near the bottom of the convective zone, thus reflecting the periodic solar activity, this requires an active/sterile mass squared difference $\Delta m_{10}^2 = O(10^{-8} eV^2)$. We therefore seek for a set of values of Δm_{10}^2 and the 8B flux normalization factor f_B which provides a good fit for both Ga I and Ga II with other solar data, together with a conveniently chosen field profile in each situation. The peak field value may be as high as $(3 - 5) \times 10^5 G$ [24], [32] at the bottom or just below the convective zone in the high activity phase corresponding to Ga II and much smaller in the semiquiet one (Ga I).

Hence we were lead to the following choice of field profile for the active phase, Ga II (1998-03) (solid line in fig.1)

$$B = \frac{B_0}{ch[10(x - x_c)]} \quad x_r < x < x_c \quad (3)$$

$$B = \frac{B_0}{ch[13(x - x_c)]} \quad x_c < x < x_r \quad (4)$$

with $x_r = 0.15$, $x_c = 0.70$ and a peak value $B_0 = 220 kG$. We take throughout the pp modulation dominance case $\Delta m_{10}^2 = -6.0 \times 10^{-9} eV^2$ and $f_B = 1.0$. With these choices pp neutrino resonances lie in the range $0.66 < x < 0.74$ centered near the peak field value at x_c , whereas the main 7Be line resonance is located at $x = 0.82$ where the field strength is $B \simeq 0.38B_0$. So the pp modulated case also has a non-negligible contribution from 7Be modulation: otherwise, if the time variation were due solely to pp resonances with a negligible field at 7Be ones even in the active period, this would imply an exceedingly fast falling field in the radial direction, thus worsening the fits.

For the semiquiet phase, Ga I (1991-97), we find the following best choice of field profile (dashed line in fig.1)

$$B = \frac{B_0}{ch[30(x - x_c)]} \quad x_r < x < x_c \quad (5)$$

$$B = \frac{B_0}{ch[15(x - x_c)]} \quad x_c < x < x_r \quad (6)$$

with $x_r = 0.25$, $x_c = 0.71$ and $B_0 = 30 kG$. This is quite similar to the previous one, the main difference being the peak value. The predictions for the 6 rates obtained in the pp modulation dominance in the active and semiquiet period are shown in table III. They all lie within 1σ of their central values except for R_{NC} lying at 1.7σ (see table III). We note a Ga rate change in a slight excess of 2σ , all other rates being approximately constant with

the possible exception of Cl whose variation is nevertheless well within 1σ . In tables III and IV the difference $\chi_{gl}^2 - (\chi_{SK_{sp}}^2 + \chi_{SNO}^2)$ is the χ^2 corresponding to the Ga and Cl rates.

| B ₀ (G) | Ga | Cl | SK | SNO _{NC} | SNO _{CC} | SNO _{ES} | $\chi_{SK_{sp}}^2$ | χ_{SNO}^2 | $\chi_{gl}^2/82$ d.o.f. |
|--------------------|------|------|------|-------------------|-------------------|-------------------|--------------------|----------------|-------------------------|
| 220 kG | 59.6 | 2.67 | 2.26 | 5.66 | 1.56 | 2.23 | 46.4 | 48.9 | 96.4 |
| 30 kG | 73.7 | 2.76 | 2.27 | 5.66 | 1.56 | 2.24 | 46.8 | 49.1 | 97.2 |

Table III - Peak field values and rates for pp modulation dominance in the active period (1998-03) (2nd row) and semiquiet period (1991-97) (3rd row). These correspond to field profiles (3), (4) and (5), (6) respectively and $\Delta m_{10}^2 = -6.0 \times 10^{-9} eV^2$. $\chi_{SK_{sp}}^2$ refers to electron scattering spectrum and χ_{SNO}^2 to charged current day/night spectrum with in addition the 4 day/night ES and NC total rates. Units are SNU for Ga, Cl and $10^6 \text{ cm}^{-2} \text{ s}^{-1}$ for SK and SNO. See tables I, II for a comparison.

3.2 Modulation by pp and ${}^7\text{Be}$

The *best* field profiles are in this case the same as the previous ones, the difference from the former case lying in the parameter Δm_{10}^2 which now satisfies $\Delta m_{10}^2 = -1.0 \times 10^{-8} eV^2$. All resonances are shifted to higher densities with the pp ones located at $0.61 < x < 0.67$ and the main ${}^7\text{Be}$ one at $x = 0.76$. With this choice ${}^7\text{Be}$ neutrinos have their resonance where the field strength is approximately 75% of its maximum. From table IV, where the rate predictions are shown for this case, it is seen that the change in the Cl rate is now larger than in the former, owing to the change in ${}^7\text{Be}$ suppression, being however smaller than 1σ . We also note a Ga rate change in excess of 2σ as in the former case.

Finally, the SuperKamiokande electron scattering spectrum and the SNO charged current one are shown respectively in figs.2 and 3 for the active sun: they are practically coincident in the scale of figs.2 and 3 for both modulations considered and close to the LMA ones.

| B ₀ (G) | Ga | Cl | SK | SNO _{NC} | SNO _{CC} | SNO _{ES} | $\chi_{SK_{sp}}^2$ | χ_{SNO}^2 | $\chi_{gl}^2/82$ d.o.f. |
|--------------------|------|------|------|-------------------|-------------------|-------------------|--------------------|----------------|-------------------------|
| 250 kG | 60.5 | 2.53 | 2.26 | 5.65 | 1.56 | 2.23 | 45.9 | 48.8 | 95.1 |
| 50 kG | 73.6 | 2.75 | 2.27 | 5.67 | 1.57 | 2.24 | 46.5 | 49.1 | 96.9 |

Table IV - Same as table III for the shared pp and ${}^7\text{Be}$ modulation dominance. Here $\Delta m_{10}^2 = -1.0 \times 10^{-8} eV^2$.

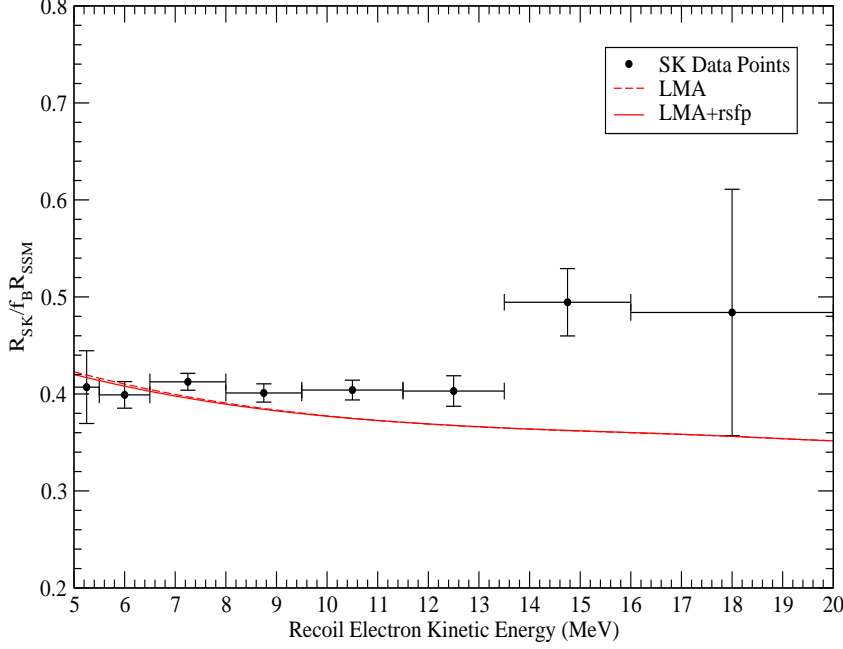


Figure 2: *SuperKamiokande* spectrum normalized to its *BS05(OP)* standard solar model [31] value with normalization factor $f_B = 1.0$. The typical spectrum predicted by the model (full curve) is close to the *LMA* one (dashed curve).

4 Borexino and LENS

Real time low energy solar neutrino experiments, monitoring pp and ${}^7\text{Be}$ fluxes in a well resolved manner, may test the possible time variability of these fluxes as hinted by the Gallium results, thus providing conclusive evidence of the neutrino magnetic moment. For this and other important reasons [14], their need was emphasized in the introduction. In this section we present our predictions for Borexino [18] and LENS [20], [21] experiments.

4.1 Borexino

Borexino is a real time organic liquid scintillator detector at Gran Sasso aimed at measuring the ${}^7\text{Be}$ flux from the sun. Extremely high radiopurity and very low background will allow

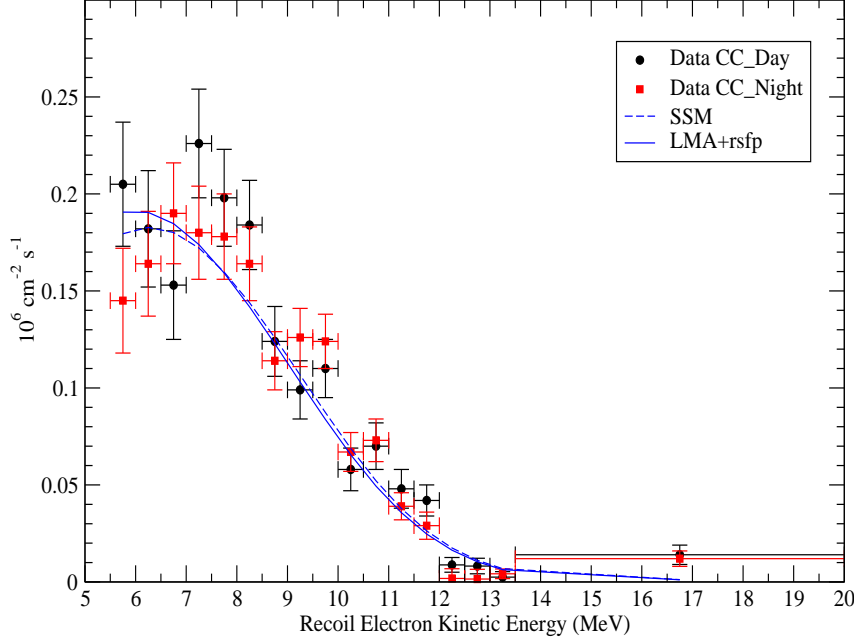


Figure 3: *SNO charged current spectrum: the model spectrum for all cases (denoted LMA+RSFP) and the LMA one are practically coincident. SSM denotes the spectrum for standard neutrinos.*

the detection of record low energy recoil electrons. The detection reaction is the neutrino scattering on electrons with a kinetic energy threshold of 250 keV and a maximum of 664 keV [18]. After some technical and environmental problems which caused several year delays, water filling is expected to start in the near future and be completed by the end of 2005. Liquid scintillator filling will then follow, so that Borexino is expected to start data taking late next year ¹. The Borexino collaboration aims at a 10% total statistical and systematic error after one year of run with an improvement to 5% after three years.

We focus our discussion on the dependence of the Borexino event rate on the peak field B_0 shown in fig.4 for the field profiles considered in section 3, from a vanishing field up to a maximum $B_0 = 300kG$. We note that for decreasing solar activity, the requirement of good fits implies a continuous shift in the profile ($1 \rightarrow 2$). For simplicity in fig.4 we show

¹For a discussion of the general treatment of our Borexino predictions we refer to reader to [33].

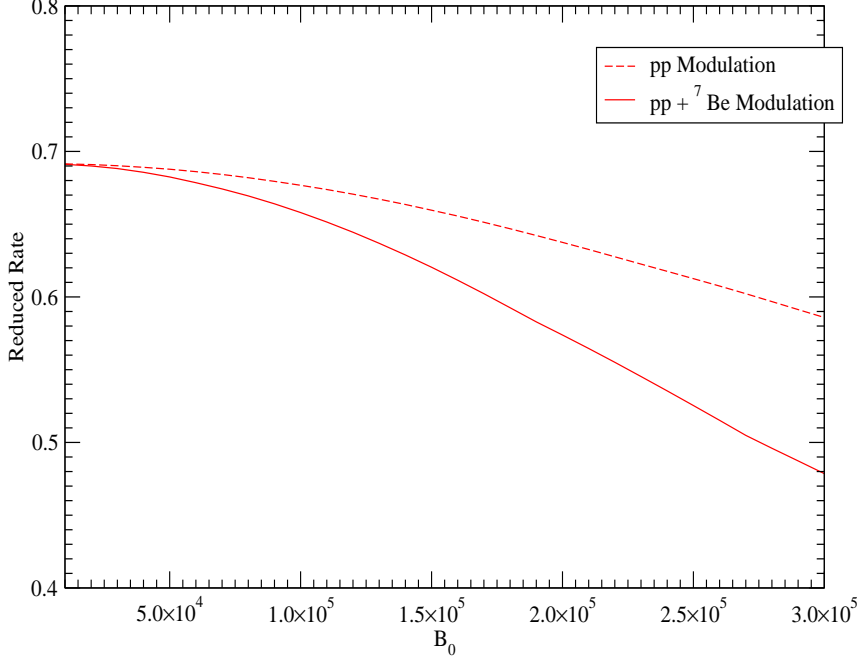


Figure 4: *Reduced Borexino event rate as a function of the peak field value (in Gauss) for profile 1.*

the curves for profile 1. We recall that the 'pure' LMA solution corresponds to $B_0 = 0$, so $R_{Bor} = 0.69$, as seen from the figure. It is also seen that in the $pp + ^7\text{Be}$ dominated modulation the rate decreases faster for increasing B_0 , thus exhibiting more sensitivity to solar activity, than in the pp case. In fact for pp dominated modulation the Borexino reduced rate varies from 0.69 at $B_0 = 0$ to 0.59 at $B_0 = 300 \text{ kG}$ (0.63 at $B_0 = 220 \text{ kG}$), while for $pp + ^7\text{Be}$ it becomes 0.48 at $B_0 = 300 \text{ kG}$ (0.53 at $B_0 = 250 \text{ kG}$). This is to be expected, as Borexino is principally directed at the ^7Be flux: the more sensitive this flux is to the peak field, correlated to solar activity, the more sensitive will the Borexino rate be. It is therefore seen that owing to the size of the experimental errors involved, the active sun (LMA+RSFP) regime may be clearly distinguishable from the quiet sun (or pure LMA) both for pp and $pp + ^7\text{Be}$ dominated modulation.

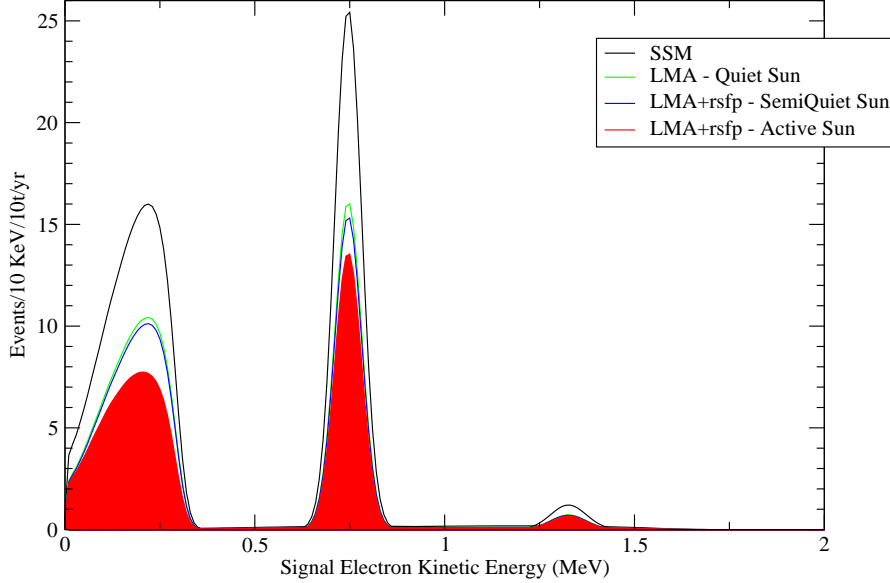


Figure 5: *Spectral LENS event rates as a function of the measured electron energy. The upper line (solid) refers to standard neutrinos (no oscillation and no spin flavour precession). The two middle ones refer to LMA and LMA+RSFP with a peak field value of 50 kG as considered in the so-called semiquiet case in section 3. The lower line refers to LMA+RSFP with peak field 220 kG. In both LMA+RSFP cases the pp dominated modulation is considered (see section 3.1).*

4.2 LENS

LENS is a real time detector measuring solar neutrinos through the charged current reaction

$$\nu_e + {}^{115}\text{In} \rightarrow {}^{115}\text{Sn} + e^- \quad (7)$$

with the lowest threshold yet: $Q=114$ keV [19], [20]. Indium was originally proposed in 1976 [19] for solar neutrino detection. Because of the low threshold, the reaction facilitates access to most of the pp continuum. The main technical problem to be solved concerns the background from the natural radioactivity of the Indium target itself. Significant progress in this problem has been made in recent years due to advances in the liquid scintillator technology [21]. Further design innovations in 2004 have advanced the project beyond the

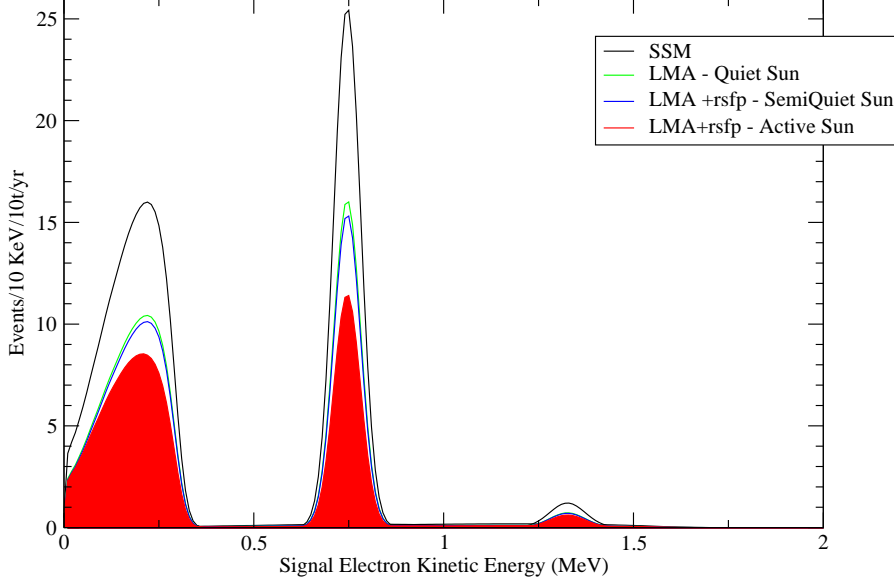


Figure 6: *The same as fig.5 for the $pp + {}^7\text{Be}$ dominated modulation (see section 3.2) with a peak field value 250 kG for the lower line.*

stage reported in ref. [21].

The charged current reaction (7) yields a particularly transparent spectrum, since the signal energy is directly and uniquely related to the neutrino energy. A resolved spectrum of all low energy components (pp , ${}^7\text{Be}$, pep , CNO) can be obtained that qualitatively shows how the sun shines.

We have calculated the event rate for the LENS detector in the case of vanishing magnetic field ('pure' LMA) and our model profile 1 with LMA for pp modulation dominance ($\Delta m_{10}^2 = -6.0 \times 10^{-9} \text{eV}^2$) and $pp + {}^7\text{Be}$ modulation dominance ($\Delta m_{10}^2 = -1.0 \times 10^{-8} \text{eV}^2$). As in Borexino, for profiles 1 and 2 the results are practically indistinguishable. The LENS event rate in the model is

$$R_{LENS} = \int_Q^{E_{max}} P_{ee}(E) f(E'_e, E_e) \phi(E) dE. \quad (8)$$

Here E is the neutrino energy, E'_e is the prompt (physical) electron energy ($E'_e = E - Q$), $f(E'_e, E_e)$ is the Gaussian energy resolution function with $\sigma = \frac{\sqrt{NE'_e}}{N}$, N being the signal

electron rate/MeV/yr. Gaussian resolution functions and detection efficiencies (for optimum signal/bgd ratios) in current design configurations have been used. The function $\phi(E)$ represents the standard spectral flux for pp , ${}^7\text{Be}$, CNO , pep neutrinos and P_{ee} is the survival probability. We used detector efficiencies $\epsilon = 0.35, 0.85, 0.80, 0.90, 0.90$ for pp , ${}^7\text{Be}$, N , O , pep neutrinos respectively. LENS event rates are shown in tables V, VI and figs.5, 6.

| | pp | ${}^7\text{Be}$ | pep | ${}^{13}\text{N}$ | ${}^{15}\text{O}$ |
|----------------------|-------|-----------------|-------|-------------------|-------------------|
| Standard | 333.2 | 226.2 | 14.22 | 9.97 | 15.48 |
| LMA | 211.6 | 138.3 | 8.30 | 6.12 | 9.24 |
| LMA+RSFP (semiquiet) | 211.1 | 137.9 | 8.29 | 6.10 | 9.22 |
| LMA+RSFP (active) | 171.3 | 120.5 | 7.83 | 5.17 | 8.34 |

Table V - LENS event rates in pp dominated modulation. Units are in events/10 t/yr. Parameters are as in section 3.

| | pp | ${}^7\text{Be}$ | pep | ${}^{13}\text{N}$ | ${}^{15}\text{O}$ |
|----------------------|-------|-----------------|-------|-------------------|-------------------|
| Standard | 333.2 | 226.2 | 14.22 | 9.97 | 15.48 |
| LMA | 211.6 | 138.3 | 8.30 | 6.12 | 9.24 |
| LMA+RSFP (semiquiet) | 211.4 | 136.2 | 8.26 | 6.04 | 9.16 |
| LMA+RSFP (active) | 184.8 | 101.5 | 7.29 | 4.50 | 7.51 |

Table VI - LENS event rates in $pp + {}^7\text{Be}$ dominated modulation. Units are in events/10 t/yr. Parameters are as in section 3.

Table V, fig. 5 are for pp modulation dominance and table VI, fig.6 for $pp + {}^7\text{Be}$ modulation dominance, all with the parameter values as fixed in section 3. In figs.5, 6 the upper curves display the standard neutrino event rates ($P = 1$), middle curves display the 'pure' LMA (quiet sun) and LMA+RSFP event rates in the semiquiet sun regime which are practically coincident as can be seen from the tables. The lower curves are for the LMA+RSFP rates in the active regime. Here the relatively low value of the pp rate is implied by the small detection efficiency ($\epsilon = 0.35$) for pp neutrinos, and the energy spread seen for ${}^7\text{Be}$ is originated from the energy resolution function. We also note the 0.114 MeV shift toward lower energies of the event rate curve relative to the solar spectrum.

From figs.5 and 6 it is seen that in both cases of study considered in section 3, for a field of the order of 200 kG in the tachocline the effect of a neutrino endowed with a magnetic moment is clearly visible in LENS. We recall that the cases considered, which are defined

by the value of the parameter Δm_{10}^2 , span the whole range of 'preferred' fits to the existing data in a model with a field profile which peaks at the tachocline. In both cases (pp and $pp + {}^7\text{Be}$ modulation dominance) the variation in the event rate from active sun, assumed to correspond to a tachocline field of 200 kG, to semiquiet or quiet (50 kG or less) produces a strong effect in the data and is of similar size in both pp and ${}^7\text{Be}$ sectors.

5 Discussion

In this paper we interpreted the Ga solar neutrino data as providing a hint for long term variability of the active solar neutrino flux in possible anticorrelation with sunspot activity and attempted at deriving its possible consequences for future experiments, namely Borexino and LENS. The claim for such long term variability was first made for the Cl experiment years ago [34],[35], [36], but later turned out to be based on invalid arguments [37], [38]. The Cl event rate is dominated by high energy neutrinos ($E > 5\text{MeV}$) to more than 75% and the more recent SuperKamiokande experiment, monitoring only these high energy ones, did not find any such effect. Long term variability, if it exists, is therefore more likely to appear in the low energy sector and its possible observation would provide evidence of new physics in connection with the neutrino magnetic moment. So far Ga experiments are the only ones having detected the low energy pp and ${}^7\text{Be}$, and they provide some evidence (see table I) of a time varying decay rate which could be associated to the solar cycle. However pp neutrinos, although overwhelming in the solar flux, only provide for approximately 55% of the Ga rate, so their possible time variation, would be partially 'erased' from the signal, as they are only seen in an inclusive measurement. The same argument applies to ${}^7\text{Be}$ neutrinos accounting for 26% of the rate.

We therefore need real time low energy solar neutrino experiments able to observe individually each neutrino component of the spectrum. As the LMA solution is based on our incomplete knowledge of the solar neutrino spectrum, one should be prepared for surprises in the future. In the previous sections we listed the main questions left open by the LMA solution (time variability, too high Cl rate, upturn in the spectrum) and summarized our previous model addressed at them using LMA and spin flavour precession to light sterile neutrinos. We attempted at fits to data treating separately the 'high' and 'low' Ga rate with a magnetic field profile exhibiting a single peak at the bottom or just below the convective zone ($x = 0.7R_S$). We found all rates to be consistent with their 1σ range except the SNO neutral current one at 1.7σ . Also our prediction for the SuperKamiokande spectrum shows the same upturn as the LMA one (see fig.2). Concerning this point it should be emphasized that the present sensitivity is not enough to make a statistically significant statement. Moreover, decreasing the spectrum upturn would require a second field peak at

around $0.9 R_S$ which is strongly disfavoured. Therefore this aspect should be left open for future clarification from the SNO experiment.

We considered time variability associated with the occurrence of either the pp or $pp + {}^7\text{Be}$ neutrino resonant transition to sterile ones in the region of the strong and varying field expected at $x = 0.7R_S$. The location of this resonance is fixed by the active/sterile mass squared difference which must lie in the range $(0.6 - 1.0) \times 10^{-8} \text{eV}^2$. Our predictions for Borexino and LENS show that these experiments have the potential of clearly identifying these solutions at least in the active solar periods, distinguishing them from the ‘pure’ LMA ones.

Finally, the proposed mechanism of $\nu_e \rightarrow \nu_s$ conversion is likely to play an important role in supernova dynamics. Its net result is expected to be the production of a neutron rich environment, thus facilitating the r-process [39], [40]. In fact, in the absence of such conversion, the reaction $\nu_e n \rightarrow p e^-$, will play an important role and will lead to the production of alpha particles via the proton capture of more neutrons. Instead, if $\nu_e \rightarrow \nu_s$ conversion takes place, proton production is obviously decreased so that more neutrons will be made available and be rapidly absorbed by seed nuclei, providing an enhancement of r-process nucleosynthesis. The reduction in the supernova ν_e flux could probably be clearly observed in the SNO experiment through the suppression of the charged current reaction (triggered only by ν_e), while it would be less apparent in SuperKamiokande where all active neutrinos contribute to neutrino electron scattering. Furthermore the adiabaticity of the transition, requiring not only a strong magnetic field [$O(10^9 \text{ G})$] but also a smooth density profile, is more likely to be realized in the later stages of the supernova explosion.

Acknowledgements

We acknowledge a discussion with Emanuela Meroni from the Borexino Collaboration. We are also grateful to David Caldwell for pointing us the importance of conversion to steriles in the supernova dynamics. The work of BCC was supported by Fundação para a Ciência e a Tecnologia through the grant SFRH/BPD/5719/2001.

References

- [1] P. A. Sturrock, D. O. Caldwell, J. D. Scargle and M. S. Wheatland, “Power-spectrum analyses of Super-Kamiokande solar neutrino data: Variability and its implications for solar physics and neutrino physics,” arXiv:hep-ph/0501205.

- [2] P. A. Sturrock and D. O. Caldwell, “Power spectrum analysis of the Gallex and GNO solar neutrino data,” arXiv:hep-ph/0409064.
- [3] P. A. Sturrock, “Analysis of Super-Kamiokande 5-day measurements of the solar neutrino flux,” *Astrophys. J.* **605**, 568 (2004) [arXiv:hep-ph/0309239].
- [4] D. O. Caldwell and P. A. Sturrock, “New evidence for neutrino flux variability from Super-Kamiokande data,” arXiv:hep-ph/0309191.
- [5] P. A. Sturrock and M. A. Weber, “Comparative analysis of GALLEX-GNO solar neutrino data and SOHO/MDI helioseismology data: Further evidence for rotational modulation of the solar neutrino flux,” *Astrophys. J.* **565**, 1366 (2002) [arXiv:astro-ph/0103154].
- [6] J. Schechter and J.W.F. Valle, *Phys. Rev.* **D24** 1883 (1981); C.S. Lim and W.J. Marciano, *Phys. Rev.* **D37** 1368 (1988); E.Kh. Akhmedov, *Yad. Fiz.* **48** 599 (1988) [*Sov. J. Nucl.Phys.* **48** 382 (1988)]; *Phys. Lett. B* **213** 64 (1988).
- [7] S. Fukuda *et al.* [Super-Kamiokande Collaboration], “Determination of solar neutrino oscillation parameters using 1496 days of Super-Kamiokande-I data,” *Phys. Lett. B* **539**, 179 (2002) [arXiv:hep-ex/0205075].
- [8] B. Aharmim *et al.* [SNO Collaboration], “Electron energy spectra, fluxes, and day-night asymmetries of B-8 solar neutrinos from the 391-day salt phase SNO data set,” arXiv:nucl-ex/0502021.
- [9] V. N. Gavrin [SAGE Collaboration], “Measurement of the solar neutrino capture rate in SAGE and the value of the pp-neutrino flux at the earth,” *Nucl. Phys. Proc. Suppl.* **138**, 87 (2005).
- [10] J. N. Abdurashitov *et al.* [SAGE Collaboration], “Measurement of the solar neutrino capture rate by the Russian-American gallium solar neutrino experiment during one half of the 22-year cycle of solar activity,” *J. Exp. Theor. Phys.* **95**, 181 (2002) [*Zh. Eksp. Teor. Fiz.* **122**, 211 (2002)] [arXiv:astro-ph/0204245].
- [11] C. M. Cattadori, talk at XXI International Conference on Neutrino Physics and Astrophysics, Neutrino 2004, <http://neutrino2004.in2p3.fr/>.
- [12] T. Kirsten [GNO collaboration] “Progress in GNO” Talk at Neutrino2002, TU Muenchen, May 2002, *Nuclear Physics B (Proceedings Supplements)* **118** (2003) 33-38.
- [13] B. T. Cleveland *et al.*, “Measurement of the solar electron neutrino flux with the Homestake chlorine detector,” *Astrophys. J.* **496**, 505 (1998).

- [14] J. N. Bahcall and C. Pena-Garay, “Global analyses as a road map to solar neutrino fluxes and oscillation parameters,” *JHEP* **0311**, 004 (2003) [arXiv:hep-ph/0305159].
- [15] H. Back *et al.*, “Report of the solar and atmospheric neutrino experiments working group of the APS multidivisional neutrino study,” arXiv:hep-ex/0412016.
- [16] J. N. Bahcall, M. C. Gonzalez-Garcia and C. Pena-Garay, “Solar neutrinos before and after Neutrino 2004,” *JHEP* **0408**, 016 (2004) [arXiv:hep-ph/0406294].
- [17] See <http://www.dxlc.com/solar/solcycle.html>.
- [18] C. Galbiati [Borexino Collaboration], talk at XXI International Conference on Neutrino Physics and Astrophysics, Neutrino 2004, <http://neutrino2004.in2p3.fr/>. See also <http://borex.lngs.infn.it/>.
- [19] R. S. Raghavan, *Phys. Rev. Letters* **37**, 259 (1976).
- [20] R. S. Raghavan, “pp solar neutrino spectroscopy: Return of the indium detector,” arXiv:hep-ex/0106054.
- [21] H. Back *et al.*, in Proceedings of 5th International Conference on Neutrino Oscillations and their Origin, Tokyo, Feb 2004, ed. Y. Suzuki *et al.*, (in press), <http://www-sk.icrr.u-tokyo.ac.jp/noon2004/>.
- [22] B. C. Chauhan and J. Pulido, “LMA and sterile neutrinos: A case for resonance spin flavour precession?,” *JHEP* **0406**, 008 (2004) [arXiv:hep-ph/0402194].
- [23] G. Gratta [KamLAND Collaboration], talk at XXI International Conference on Neutrino Physics and Astrophysics, Neutrino 2004, <http://neutrino2004.in2p3.fr/>.
- [24] H. M. Antia, S. M. Chitre and M. J. Thompson, “The Sun’s acoustic asphericity and magnetic fields in the solar convection zone,” *Astron. Astrophys.* **360** 335 (2000) [arXiv:astro-ph/0005587].
- [25] B. C. Chauhan, J. Pulido and E. Torrente-Lujan, “KamLAND, solar antineutrinos and the solar magnetic field,” *Phys. Rev. D* **68**, 033015 (2003) [arXiv:hep-ph/0304297].
- [26] C. S. Lim, M. Mori, Y. Oyama and A. Suzuki, “Correlation Between Solar Neutrino Flux And Solar Magnetic Activity For Majorana Neutrinos,” *Phys. Lett. B* **243**, 389 (1990).
- [27] E. K. Akhmedov, “Anti-neutrinos from the sun,” *Phys. Lett. B* **255**, 84 (1991).

- [28] R. S. Raghavan, A. B. Balantekin, F. Loreti, A. J. Baltz, S. Pakvasa and J. T. Pantaleone, “Direct tests for solar neutrino mass, mixing and majorana magnetic moment,” *Phys. Rev. D* **44**, 3786 (1991).
- [29] K. Eguchi *et al.* [KamLAND Collaboration], “A high sensitivity search for anti- ν /e’s from the sun and other sources at KamLAND,” *Phys. Rev. Lett.* **92**, 071301 (2004) [arXiv:hep-ex/0310047].
- [30] J. Pulido, “Solar neutrinos with magnetic moment: Rates and global analysis,” *Astropart. Phys.* **18**, 173 (2002) [arXiv:hep-ph/0112104].
- [31] J. N. Bahcall and A. M. Serenelli, “New solar opacities, abundances, helioseismology, and neutrino fluxes,” *Astrophys. J.* **621**, L85 (2005) [arXiv:astro-ph/0412440].
- [32] S. Couvidat, S. Turck-Chieze and A. G. Kosovichev, “Solar seismic models and the neutrino predictions,” *Astrophys. J.* **599**, 1434 (2003).
- [33] E. K. Akhmedov and J. Pulido, “Distinguishing magnetic moment from oscillation solutions of the solar neutrino problem with Borexino,” *Phys. Lett. B* **529**, 193 (2002) [arXiv:hep-ph/0201089].
- [34] J. K. Rowley, B. T. Cleveland and R. Davis, “The Chlorine Solar Neutrino Experiment,” *AIP Conf. Proc.* **126**, 1 (1984).
- [35] M. B. Voloshin and M. I. Vysotsky, “Neutrino Magnetic Moment And Time Variation Of Solar Neutrino Flux,” *Sov. J. Nucl. Phys.* **44**, 544 (1986) [*Yad. Fiz.* **44**, 845 (1986)].
- [36] L. B. Okun, M. B. Voloshin and M. I. Vysotsky, “Electromagnetic Properties Of Neutrino And Possible Semiannual Variation Cycle Of The Solar Neutrino Flux,” *Sov. J. Nucl. Phys.* **44**, 440 (1986) [*Yad. Fiz.* **44**, 677 (1986)].
- [37] P. A. Sturrock, G. Walther and M. S. Wheatland, “Search for periodicities in the Homestake solar neutrino data,” *Astrophys. J.* **491**, 409 (1997).
- [38] G. Walther, “Reply to comment on ‘Absence of correlation between the solar neutrino flux and the sunspot number’,” *Phys. Rev. Lett.* **79**, 4522 (1997) [*Phys. Rev. Lett.* **83**, 1895 (1999)] [arXiv:astro-ph/9710031].
- [39] G. C. McLaughlin, J. M. Fetter, A. B. Balantekin and G. M. Fuller, “An Active-Sterile Neutrino Transformation Solution for r-Process Nucleosynthesis,” *Phys. Rev. C* **59**, 2873 (1999) [arXiv:astro-ph/9902106].

- [40] J. Fetter, G. C. McLaughlin, A. B. Balantekin and G. M. Fuller, “Active-sterile neutrino conversion: Consequences for the r-process and supernova neutrino detection,” *Astropart. Phys.* **18**, 433 (2003) [arXiv:hep-ph/0205029].